sciendo
Austrian Journal of Earth Sciences | Vienna | 2020 | Volume 113/2 | 211 - 226 | DOI: 10.17738/ajes.2020.0013

Late Glacial ice advance in the Kellerjoch region near Schwaz (Tyrol, Eastern Alps)

Philipp GSCHWENTNER[1], Hanns KERSCHNER[2], Christoph SPÖTL[1*]
[1] Institute of Geology, University of Innsbruck, Innrain 52, 6020 Innsbruck, Austria
[2] Institute of Geography, University of Innsbruck, Innrain 52, 6020 Innsbruck, Austria
*) corresponding author: christoph.spoetl@uibk.ac.at

KEYWORDS Pleistocene, Late Glacial, palaeoglacier, geomorphology, Gschnitz stadial

Abstract
The Kellerjoch forms a small isolated massif at the northernmost rim of the central Eastern Alps of Tyrol and shows a number of geomorphological features of glacial and periglacial origin. Mapping yields evidence of two local glaciations postdating the Last Glacial Maximum. Using a simple glaciological approach the palaeoglaciers related to these events were reconstructed. The older glaciation yields an equilibrium line altitude (ELA) ranging from 1660 m for the maximum extent to 1800 m a.s.l. for the innermost moraine. For the younger glaciation, ELAs were reconstructed at 1905 m and 1980 m (depending on the reconstruction) for the Kellerjoch palaeoglacier 2, as well as 1870 m and 2060 m a.s.l. for the Proxen palaeoglacier and the Gart palaeoglacier, respectively. A comparison with published data from the Eastern Alps shows that the older glaciation in the Kellerjoch region likely corresponds to the Gschnitz stadial. Low basal shear stresses of the glacier tongues point towards a cold and dry climate, similar to the reconstruction for the Gschnitz type locality at Trins. The younger glaciation cannot unambiguously be assigned to a specific Late Glacial ice advance, but a Younger Dryas age is a distinct possibility.

1 Introduction

The history of the last glacial period and its impact on the landscape of the Alps have been investigated intensely since many decades (see e.g. Heiri et al. (2014) for a recent overview). Of particular interest is the interval between the end of the Last Glacial Maximum (LGM) and the onset of the Holocene, the so-called Alpine Late Glacial (Fig. 1). This approximately 7 kyr-long period saw the collapse of the piedmont glaciers in the foreland of the Alps, the down wasting of the ice-stream network occupying the main valleys and basins within the Alps, the reforestation starting with the abrupt warming at 14.7 ka BP, and the 1200 yr-long cold spell of the Younger Dryas.

Recent studies show that the LGM in the Alps came to an end at 19-18 ka BP. Ice-surface lowering in the accumulation area commenced at 18.5 ± 1.1 ka in the Mont Blanc area and at 18.6 ± 1.4 ka in the Zillertal Alps (Wirsig et al., 2016). Field evidence for the down wasting of the large valley glaciers in the Eastern Alps was reported e.g. from the Hopfgarten basin in Tyrol (Reitner, 2007), where kame-terrace sediments yielded an average luminescence age of 19 ± 2 ka BP (Klasen et al., 2007). The oldest radiocarbon dates from palaeolake sediments in the area of Bad Mitterndorf (Styria) and at Längsee (Carinthia) also date from 18-19 ka BP (van Husen, 1997; Schmidt et al., 2012) as do optically stimulated luminescence dates of aeolian silt from the western Northern Calcareous Alps in Tyrol (Gild et al., 2018).

Around 17 ka BP a climate deterioration probably associated with the Heinrich 1 meltwater event in the North Atlantic caused a first major glacier re-advance after the LGM, known as the Gschnitz stadial (Kerschner et al., 1999; Ivy-Ochs et al., 2006). At the type locality at Trins (Fig. 2) in the Gschnitz valley of Tyrol, a prominent terminal and lateral moraine is preserved and ^{10}Be exposure dating indicates a stabilisation at about 15.4 ka BP (Ivy-Ochs et al., 2006). A re-calibration using ^{10}Be production rates (Balco et al., 2009; Heyman, 2014) resulted in a revised stabilisation age of 16.7 ± 1.3 ka BP (Kerschner et al., 2014). A reconstruction of the equilibrium line altitude (ELA) and its glaciological interpretation for the former Gschnitz valley glacier suggests precipitation of one third of the modern value and summer temperatures roughly 10 °C lower than today (Kerschner et al., 1999). Reconstructed low basal shear stress suggests a rather low ice flow velocity of this palaeoglacier, consistent with a cold and dry climate (Kerschner et al., 1999; Ivy-Ochs et al., 2006).

The Gschnitz re-advance was followed by a rapid warming starting at 14.7 ka BP, which led to the Bølling-Allerød-Interstadial. During this warm and humid interval, glacier

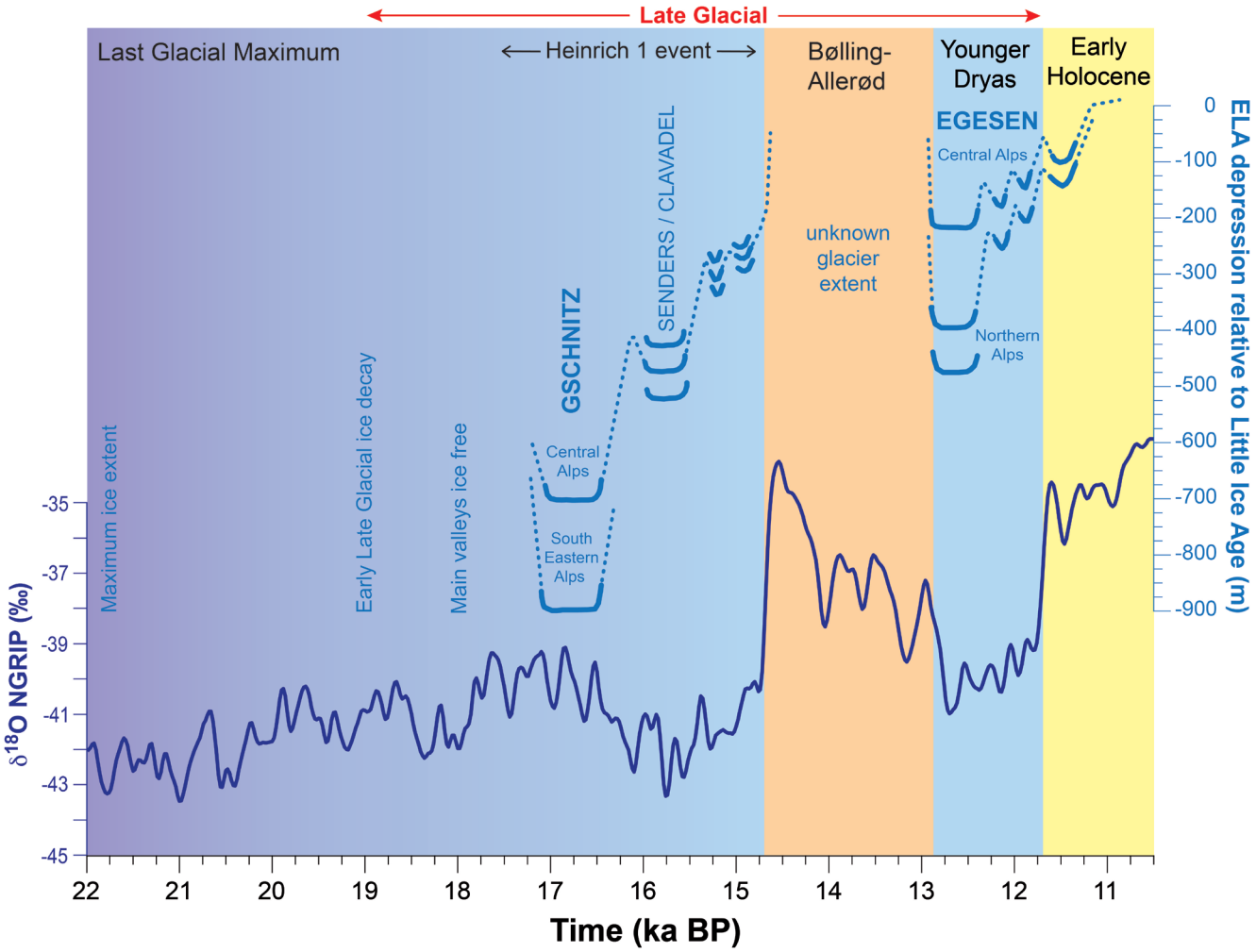

Figure 1: Chart showing the general evolution of the climate in the northern hemisphere (expressed as oxygen isotope composition of ice in the NGRIP core from Greenland) and of the glaciers in the Eastern Alps (expressed as depression of the equilibrium line altitude, ELA) from the Last Glacial Maximum across the Late Glacial into the early Holocene. Modified after Auer et al. (2014).

tongues receded considerably and the former glacial landscape became rapidly forest-covered (Bortenschlager, 1984). The Bølling-Allerød interstadial was abruptly terminated at 12.9 ka BP by the Younger Dryas (Egesen stadial). During this 1200 yr-long cold spell alpine glaciers advanced significantly and rock glaciers were also active and often originated from moraines (Ivy-Ochs et al., 2008). Moraines of the earliest and most extensive advance, the Egesen maximum, stabilised during the first half of the Younger Dryas (Ivy-Ochs et al., 2015). Climate reconstructions based on Egesen-ELA data suggest precipitation along the northern fringe of the Eastern Alps broadly similar to modern values, whereas valleys close to the main alpine crest experienced a reduction of 20 to 30 % compared to today (Kerschner et al., 2007). The cold climate of the Younger Dryas faded out during the earliest Holocene and several moraine systems in the Alps date to between about 11.6 and 10.5 ka BP (Ivy-Ochs et al., 2009; Moran et al., 2016 a, b).

This study provides geomorphological evidence of Late Glacial ice advances at the boundary between central Eastern Alps and the Northern Calcareous Alps in North Tyrol, in order to refine palaeoclimatological reconstructions in the Eastern Alps. The study site, the Kellerjoch region, shows well-preserved evidence of two Late Glacial advances of local palaeoglaciers.

2 Setting

2.1 Geology

The Kellerjoch massif forms the northeastern corner of the Tux Prealps, confined by the Ziller Valley in the East and the Inn Valley to the Northwest. The region is built up of three main geological units (Fig. 2), the Northern Calcareous Alps, the Greywacke Zone and the Innsbruck Quartzphyllite. Formations of the Northern Calcareous Alps are only present in the northernmost part of the Kellerjoch massif and are collectively known as "Schwazer Trias" (Triassic of Schwaz). This sedimentary succession ranges from the Upper Permian to the Upper Triassic. These rocks are characterised by a strong tectonic overprint, which is partly related to the movements along the Inn Valley fault which separates the "Schwazer Trias" from

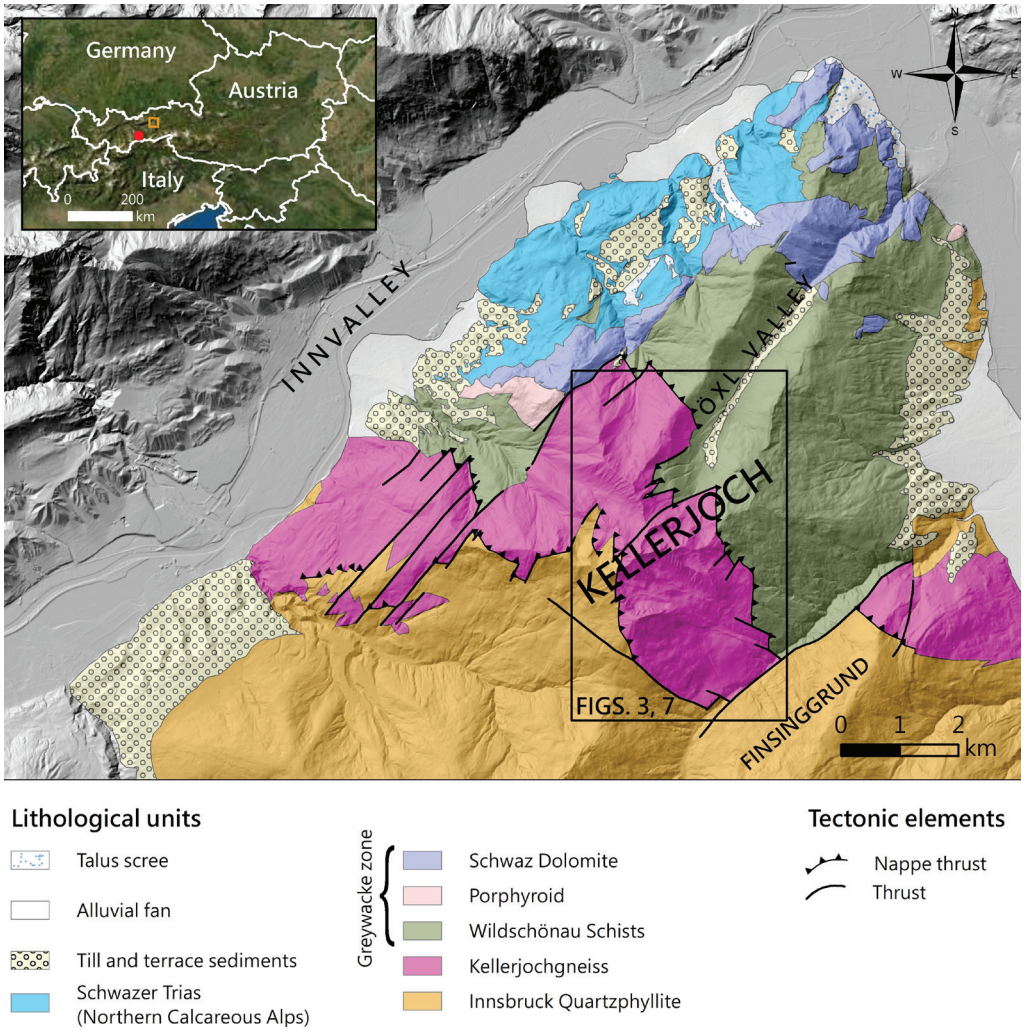

Figure 2: Generalised geologic map of the Kellerjoch region (after Moser, 2008). The black rectangle marks the areas of Figures 3 and 7. The red point in the overview map shows the location of type locality of the Gschnitz Stadial.

the main body of the Northern Calcareous Alps north of the Inn Valley.

The Greywacke Zone can be subdivided into the Wildschönau Schists and the Kellerjochgneiss. The former consist of a lower unit with intercalations of mafic and ultramafic rocks, while the upper unit contains (meta)carbonates, such as the Upper Devonian Schwaz Dolomite. The Kellerjochgneiss is a metagranitoid body of Middle Ordovician age (Tropper et al., 2016), present as augengneiss or as a highly mylonitic gneiss (''Stengelgneis''). Both Wildschönau Schists and Kellerjochgneiss were metamorphosed at lower greenschist conditions (Piber, 2005; Tropper and Piber, 2012).

The rather monotonous series of the Innsbruck Quartzphyllite ranges in age from the Ordovician to the Devonian and consists of metabasic rocks in the lower subunit, intercalations of meta-carbonates in the middle part and graphitic phyllites and ferroan meta-dolomites in the upper subunit (Haditsch & Mostler, 1982; Kolenprat et al., 1999; Rockenschaub et al., 1999). These rocks also experienced a lower to middle greenschist metamorphic overprint (Tropper and Piber, 2012).

2.2 Geomorphology

The summits of the Kellerjoch massif formed crest-shaped nunatakks during the LGM (van Husen, 1987), when the ice surface of the Inn and Ziller palaeoglaciers reached about 2000 m a.s.l. in the W, N and E. The highest summit in this crest, the Kreuzjoch, reaches an altitude of 2344 m a.s.l. The massif itself is dissected by prominent cirques oriented towards NE, E and NW (Fig. 3). The summit region is characterised by three deep-seated gravitational slope deformations (DSGSD), which were mapped and investigated by Grasbon (2001). According to Grasbon (2001), the lower boundaries of these DSGSDs are diffuse rather than discrete shear zones suggesting a diffuse sagging likely caused by the partially intense fragmentation of the bedrock.

Two prominent valleys are present in the Kellerjoch massif. The Öxl valley (Figs. 2, 3) is 7 km long, trough-shaped, with a smooth and rather flat valley floor, stretching in NNE direction. After about 5 km the valley shows a step and incised section that ends in an alluvial fan in the Ziller valley. To the SW, the Finsinggrund (Figs. 2, 3) is a curved valley with a length of about 12 km. The Finsinggrund is

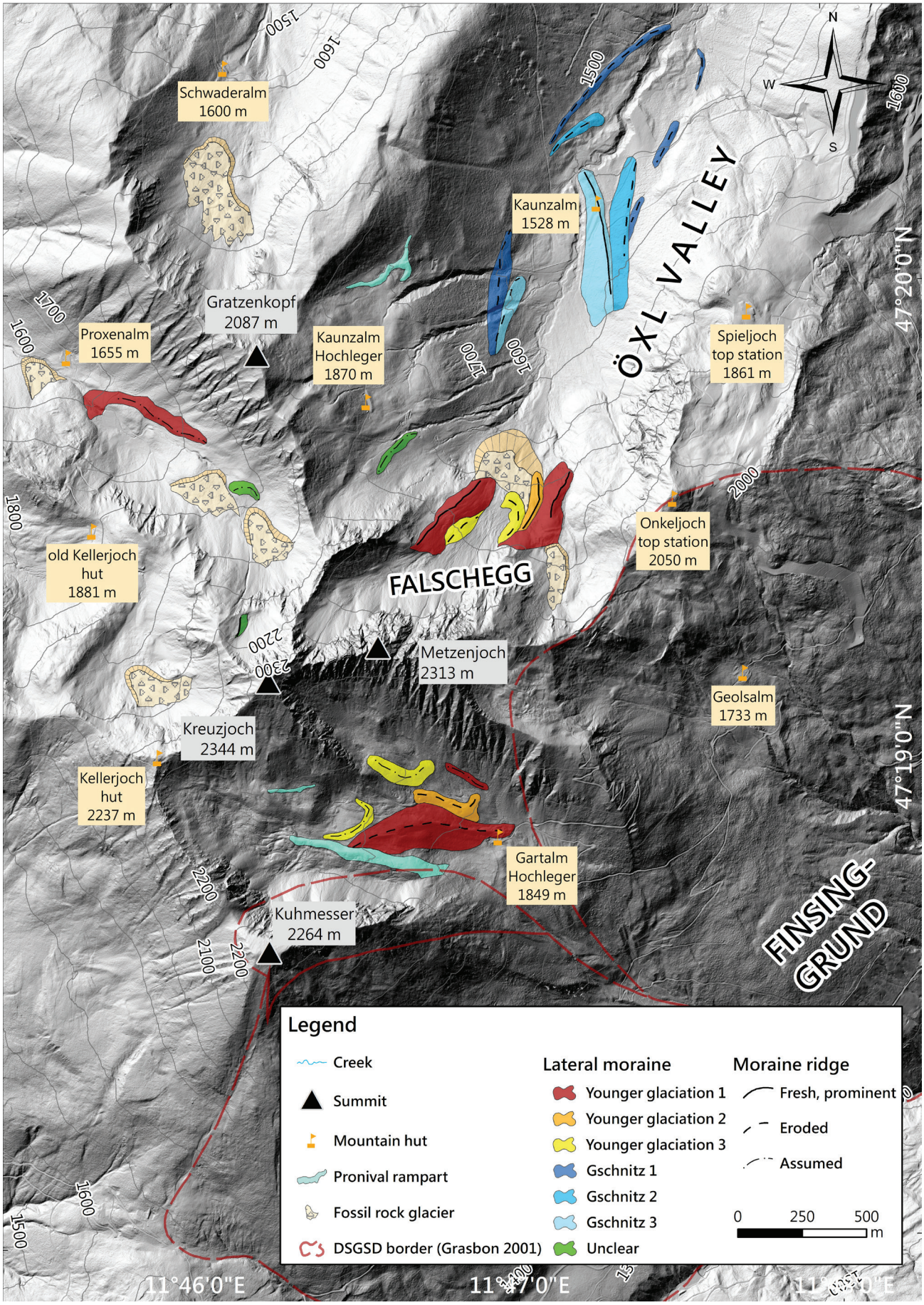

Figure 3: Geomorphologic map of the central Kellerjoch massif.

characterised by DSGSDs on the orographic left valley flank (Grasbon, 2001), but several mass movements are also present on the opposite valley side.

The Kellerjoch massif was already investigated by Klebelsberg (1951), who described several lateral and terminal moraines around the crest of the Kellerjoch. Patzelt (2019) recently published a short account on the glacial geomorphology at Kellerjoch. He reported a pentamerous moraine series, e.g. in the Öxl valley. Several smaller wall-like structures and rock glacier-like features were interpreted as terminal or lateral moraines.

3 Methods

The reconstruction of the Late Glacial glaciers in the Kellerjoch region is based on detailed field mapping aided by the interpretation of airborne laserscan images. Altitudes were determined in the field by a hand-held GPS and verified by a digital elevation model (DEM) in ArcGIS. These DEM-values were used afterwards for the reconstruction of the glacier topographies.

The ELA of the former glaciers was estimated by two methods, the maximum elevation of lateral moraines (MELM), and the accumulation area ratio (AAR) method. The first approach was developed independently by Lichtenecker (1938) and Visser (1938), who studied glaciers in the Alps and the Karakorum, respectively. It is based on the kinematic theory of glacier motion by Finsterwalder (1897). The method assumes that the highest observable position of a lateral moraine, which is not influenced by postdepositional erosion, lateral sediment cover, steep slopes or other processes, which make the preservation of the onset of a lateral moraine impossible, marks the ELA for glaciers in steady state with the climate. The second method has been widely applied in the Alps and commonly uses an AAR of 0.67 (Gross et al., 1977, Kerschner et al., 2008). This widely used method calculates the ratio of the area of the accumulation zone of a glacier to its total area, which means that in the Alps a glacier commonly needs two-thirds of its total area for accumulating precipitation to compensate for ablation.

The ice thickness of the former glaciers was assessed with a simple shear-stress model (Cuffey and Paterson, 2011). It is based on the realistic assumption that the basal shear stress at the basis of a glacier is quasi-constant. Under the assumption of perfect plasticity (Paterson, 1972), flow of ice happens only when its yield strength is exceeded and any increase in stress before reaching the yield strength only causes a further increase of stress – and not a flow of the ice. Then, the ice thickness H can be calculated from the shear stress equation as

$$H = \frac{1}{f} \cdot \frac{\tau_0}{\rho \cdot g \cdot \alpha}$$

where H is the ice thickness, f is a shape factor which accounts for the drag of the lateral valley walls, τ_0 is the basal shear stress, ρ is the ice density (900 kg m^{-3}), g is the acceleration due to gravity (9.81 m s^{-2}), and α is the surface slope of the glacier. If a sufficient stretch of lateral moraines is preserved, the basal shear stress can be determined from the height of the moraines relative to the central axis of the former glacier bed and a from the slope of the moraines parallel to the valley axis. The shape factor can be determined from the cross section of the former glacier bed. If moraines are missing, the assumption of a constant shear stress of 100 kPa can be a reasonable first-order assumption for valley glaciers (Paterson, 1972).

In practice, long profiles of the glaciers were calculated with the EXCEL-spreadsheet provided by Benn and Hulton (2010). This also allows the calculation of a shape factor for each cross section based on its hydraulic radius. This approach was originally proposed by Nye (1952). Later, Nye (1965) refined the approach by calculating shape factors for rectangular, elliptic and parabolic cross sections. However, in the case of our study, the numerical values of both approaches are very similar. By choosing points within the former glacier the ice thickness was calculated and contoured. Using these contour lines, a 3D-surface of the glacier topography was generated using GIS software.

4 Results

4.1 Moraine systems

Field work revealed evidence of four individual moraine systems: Kaunzalm, Falschegg, Proxenalm and Gartalm (Figs. 3, 4, 5, 6). Except for the area near the Proxenalm where only one distinct moraine is present, all other locations show morphological evidence of at least three subsystems, which can be distinguished in the field as well as in hillshade images. Four main areas showing morphological evidence of moraine systems are briefly characterised below.

4.1.1 Kaunzalm

The most prominent moraine system is found in the Öxl valley at the Kaunzalm. Three distinct moraine sets can be distinguished with ridge heights of up to 3 m (Figs. 3, 4). Only few boulders lie on the strongly vegetated moraines. The terminal moraine of the largest glacier subsystem (Kaunzalm A sensu Patzelt, 2019) is located at an altitude of about 1420 m and can be traced up to 1660 m on the western side, whereas the eastern part of this subsystem shows a superposition by another subsystem at about 1560 m (dark blue line Fig. 4). The front of this moraine is strongly eroded by the Öxl creek.

The moraines of the second subsystem (Kaunzalm B sensu Patzelt, 2019) also show strong weathering and only few boulders are present on the strongly vegetated and partly wooded area. The terminal moraine is located at about 1480 m and reaches up to 1630 m on the western valley side, whereas the eastern part is overlain by another smaller subsystem at about 1620 m (light blue line in Fig. 4). Lateral moraines on the western valley side are 2-3 m high and reach up to 10 m on the eastern valley side.

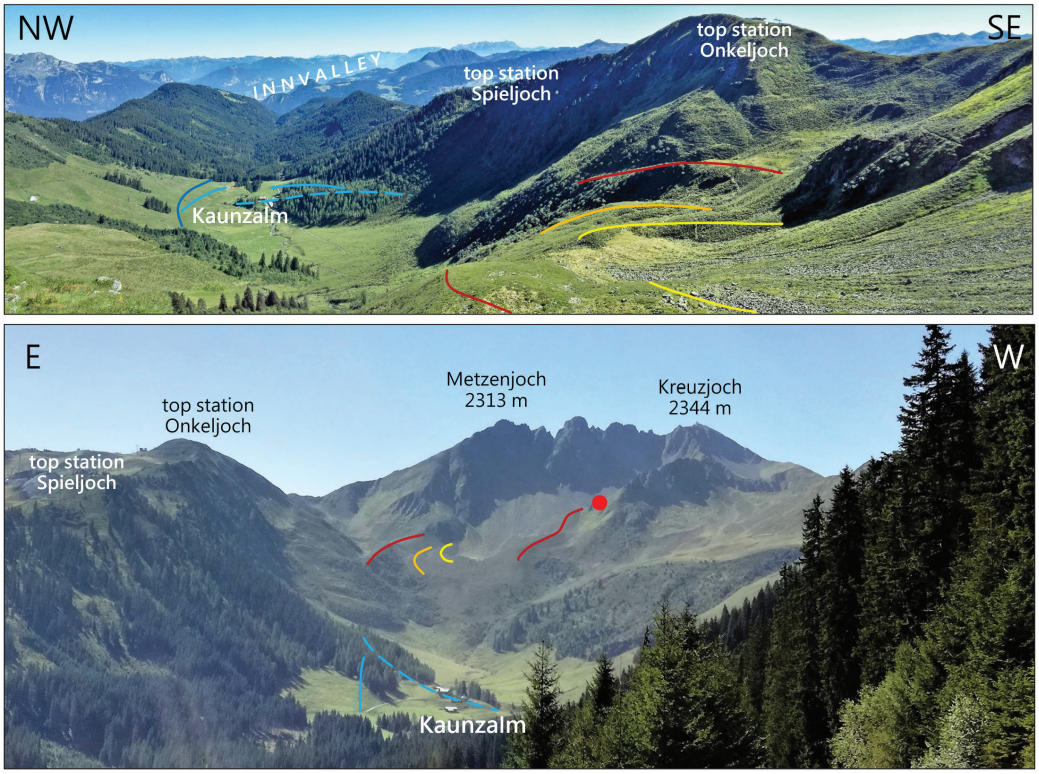

Figure 4: Overview of the moraine systems at the Kaunzalm and Falschegg. The red dot in the lower figure marks the position from where the upper picture was shot. The dark blue line indicates the largest glacier extent at the Kaunzalm, light blue shows the second moraine subsystem and the smallest subsystem is marked by the dashed light blue line. In the Falschegg cirque, the most prominent lateral moraine is indicated by the red line, whereas the lateral moraines are marked by orange and yellow lines.

The third and smallest subsystem (Kaunzalm C sensu Patzelt, 2019) was identified at the buildings of the Kaunzalm. The right-lateral moraine ridge is the most prominent feature of this system with the farmhouse sitting right on it (dashed light blue line in Fig. 4). This ridge is up to 15 m high on the eastern valley side, while the western part is poorly developed and difficult to identify. The terminal moraine is located at about 1500 m and its eastern part can be traced to about 1620 m, whereas the subtle western part reaches up to about 1650 m.

4.1.2 Falschegg

Another moraine system exists further up valley in the Falschegg cirque (Fig. 4). Again, three sets of moraines can be distinguished (Figs. 3, 4). The most prominent one can be traced from its terminus at about 1680 - 1700 m to the uppermost lateral moraine at about 1990 m (red line in Fig. 4). A second smaller lateral moraine can be traced from about 1770 m to about 1860 m, where it is covered by talus scree (orange line in Fig. 4). The terminus of this system is indistinct and grades into a rock glacier-like landform, which may be interpreted as a glacier-rock glacier continuum (Kaunzalm D sensu Patzelt 2019). The smallest moraine in the Falschegg cirque is strongly weathered but still can be clearly identified (yellow line in Fig. 4). The terminal moraine lies at an altitude of about 1820 m and the lateral moraine can be traced to about 1880 m. On the small Spieljoch plateau, a rock glacier formed in front of a glacieret or perennial snow patch, which probably developed contemporaneously with the system to the north of Metzenjoch described above. Patzelt (2019) assigned the landform to his phase D. Possible older landforms were destroyed during the construction of the Spieljoch cable car.

4.1.3 Proxenalm

A prominent right-lateral moraine ridge is present near the Proxenalm, including a well-developed terminal moraine (red line in Fig. 5) located at 1680 m altitude. The right-lateral moraine can be traced up to an altitude of 1840 m and is then overlain by talus scree. The former glacier end is partly obscured on the left-hand side by the lower part of a gravitational slope failure. Patzelt (2019) correlated this moraine with the B-moraine at Kaunzalm and paralleled a small, rock glacier like structure downvalley of the slope failure with Kaunzalm A.

Further up, a smaller and less prominent ridge can be observed at about 1900 m showing a characteristic morphology of a terminal moraine (orange line in Fig. 5, green area in Fig. 3). Finally, in the uppermost part of the cirque immediately to the North of Kellerjoch summit, a lateral moraine of a small glacier can be found with an upper end at 2180 m. The end of the glacier, which seems to have been mainly fed by wind drift and avalanches, was most probably at the upper edge of the rocky step leading down to Proxenalm at 2140 m. It is the stadial F of Patzelt (2019). He also assigned a structure in the cirque

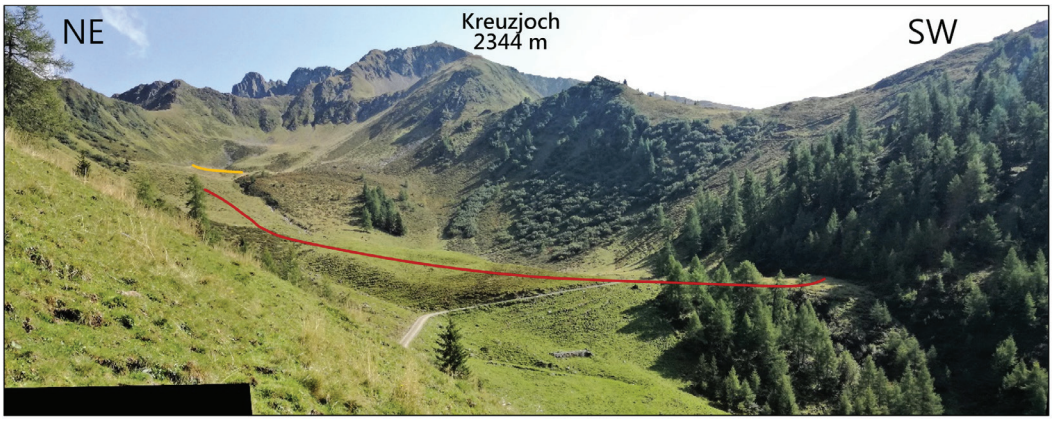

Figure 5: Overview of the morainal systems above the Proxenalm. The red line marks the prominent lateral moraine, which merges with a terminal moraine near its front. The orange line marks a small ridge at about 1900 m.

immediately to the W of Kellerjoch in the headwaters of Talzlbach to the stadial F, which we would rather like to interpret as a rock glacier that developed in front of a perennial snow patch. In the adjacent Talzlbach valley, Patzelt (2019) further mapped a moraine sequence of stadials A to D, whereas a stadial B was apparently not identified by him. In our study, we did not consider this area in further detail, due to remaining ambiguity.

4.1.4 Gartalm

Three separate moraines can be distinguished in the cirque above the Gartalm (Figs. 3, 6). The terminus of the most prominent one is located right above the hut at 1850 m altitude. This right-lateral moraine can be followed up to 2010 m, where it is overlain by a straight, distinct ridge (red line in Fig. 6). On the orographic left side, a corresponding subtle ridge was identified within the talus (red dashed line in Fig. 6). A second, smaller lateral moraine lies only a few metres above the most prominent lateral moraine (orange line in Figs. 3, 6). Parts of its terminus are located at about 1880 m and can be traced up to about 1960 m. A corresponding left-lateral moraine was not identified. A third and subtle right-lateral moraine is located at about 1960 m in a small side valley beneath the summit of the Kreuzjoch (dashed yellow line in Fig. 6) and can be traced up to about 2055 m; no corresponding left-lateral features exist there. A curved flat ridge is present in the main cirque, located at about 2010 m (yellow dashed line in Fig. 6).

4.2 Palaeoglacier reconstruction

Based on the mapping results, four palaeoglaciers at Kaunzalm (Kellerjoch palaeoglacier 1), Falschegg (Kellerjoch palaeoglacier 2), Proxenalm (Proxen palaeoglacier) and Gartalm (Gart palaeoglacier) were identified (Fig. 7). Within each moraine system the palaeoglaciers with the largest extent were reconstructed, at Kaunzalm also the two smaller glacier extents were included. Table 1 shows the main results of each reconstructed palaeoglacier and Table 2 provides various parameters for the calculation of the ice thickness of each reconstruction point.

Kellerjoch palaeoglacier 1 is the largest and longest with a length of about 3 km long. Ten points were chosen for the ice thickness calculation, which yielded values between 38 m (FA2) and 93 m (KZ1). Yield strength was adapted depending on the steepness at the location of the calculation point and varies between 50 and 150 kPa. At certain points also a shape factor was determined, ranging from 0.56 to 1.

Calculations of the palaeo-ELA based on the MELM-method and using an AAR of 0.67 typical of alpine glaciers (Gross et al., 1977; Kerschner et al., 2008) yielded altitudes

Palaeoglacier	Exposition	Highest altitude [m a.s.l.]	Lowest altitude [m a.s.l.]	Length [km]	ELA by MELM		ELA with AAR=0.67 [m a.s.l.]	ELA difference [m a.s.l.]
					Altitude [m a.s.l.]	AAR		
Kellerjoch palaeoglacier 1	NNE	2200	1414	3	1660	0.66	1650	10
Kellerjoch palaeoglacier 2	NE	2203	1700	1.3	1990	0.51	1905/1980*	85/10*
Proxen palaeoglacier	NW	2225	1725	1.3	1840	0.74	1870	30
Gart palaeoglacier	SE	2175	1850	1.3	2010	0.81	2060	50

* With and without debris-covered part of glacier tongue

Table 1: Glaciological parameters of the reconstructed Kellerjoch palaeoglaciers.

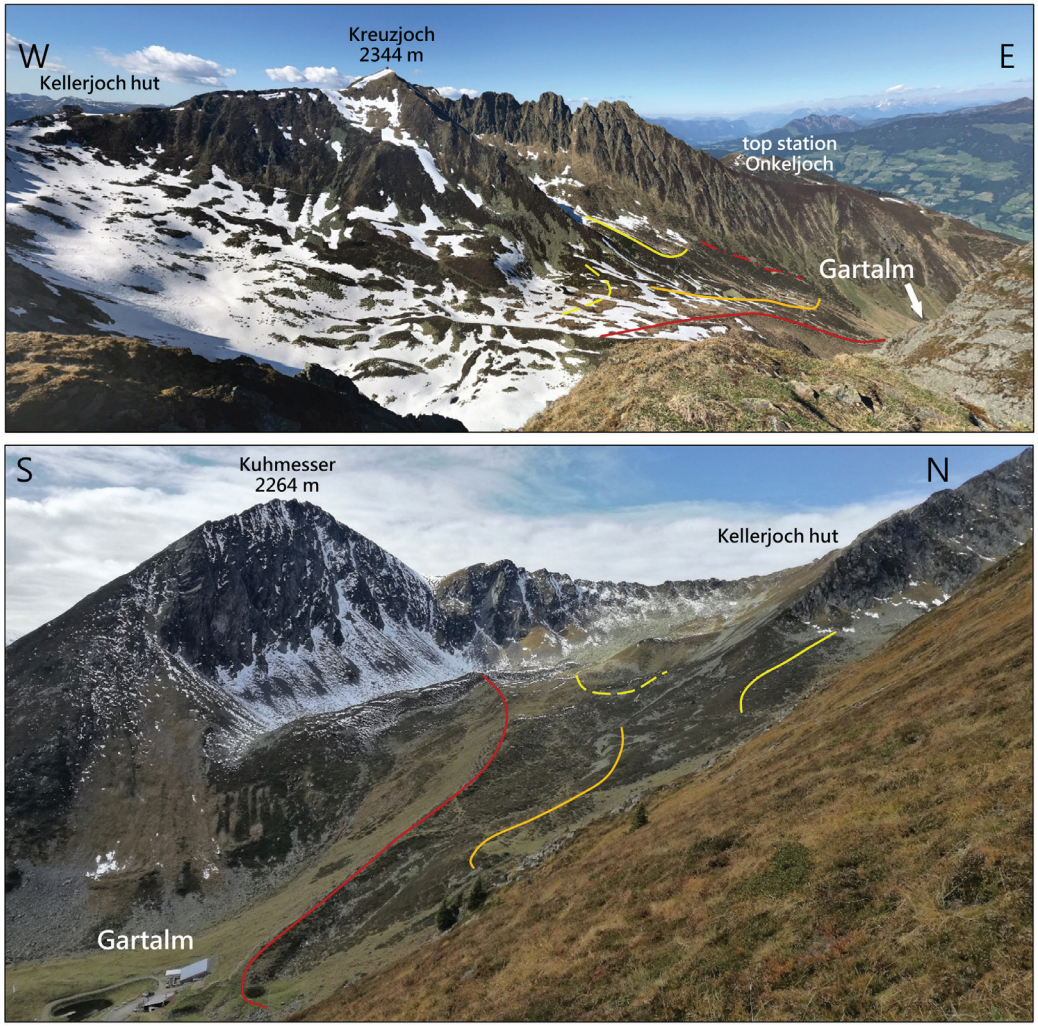

Figure 6: Three moraine ridges can be distinguished in the Gartalm cirque. The red line marks the most prominent lateral moraine. A probably corresponding subtle ridge was identified in the talus and is indicated by a dashed red line. The orange line marks a second subsystem and the yellow line shows the smallest feature in this cirque. The dashed yellow line delineates a further subtle ridge, which likely corresponds to the smallest glacier extent in this cirque.

of 1660 m (AAR = 0.66) and 1650 m, respectively, for the maximum extent (Kaunzalm A). The ELAs (AAR = 0.67) of Kaunzalm B and C were located at 1700 m and 1800 m, respectively.

Kellerjoch palaeoglacier 2 in the Öxl valley was 1.2 km long. Three calculation points yielded ice thickness values between 34 m (KG7) and 69 m (KG9). Yield strength was chosen between 125 and 130 kPa, given the rather constant slope. Shape factors were adapted from Kellerjoch palaeoglacier 1. Palaeo-ELA estimations yielded altitudes of 1990 m (AAR = 0.51, MELM-method) and 1905 m (AAR = 0.67) with the inclusion of the debris-covered lower part of the glacier tongue. If the debris-covered part of the tongue is excluded, an AAR of 0.67 results in an ELA of 1980 m, which agrees with the results from the MELM-method.

Proxen palaeoglacier was reconstructed above the Proxenalm with a length of 1.3 km. Four points were used to determine its ice thickness and the values are between 37 m (PR3) and 80 m (PR2). A value between 125 kPa and 150 kPa was chosen for the yield strength in an especially steep part of the glacier. Three shape factors were calculated, ranging from 0.60 to 0.65. The palaeo-ELA was located between 1840 m (AAR = 0.74) and 1870 m (AAR = 0.67).

Gart palaeoglacier was reconstructed as the fourth palaeoglacier with a length of about 1.3 km. Four points for determining the ice thickness yielded values between 59 m (GA1) and 88 m (GA3). Yield strength varied between 125 kPa and 130 kPa. Due to the similarity of the valley shape, three of four shape factors were taken from the Proxen palaeoglacier, ranging from 0.62 to 0.67. The palaeo-ELA was located between 2010 m (MELM-method, AAR = 0.81) and 2060 m (AAR of 0.67).

4.3 Permafrost features

4.3.1 Fossil rock glaciers

Four fossil rock glaciers were mapped in the cirques of the Kellerjoch massif (Fig. 3, parameters are given in Table 3). All rock glaciers show typical morphological features,

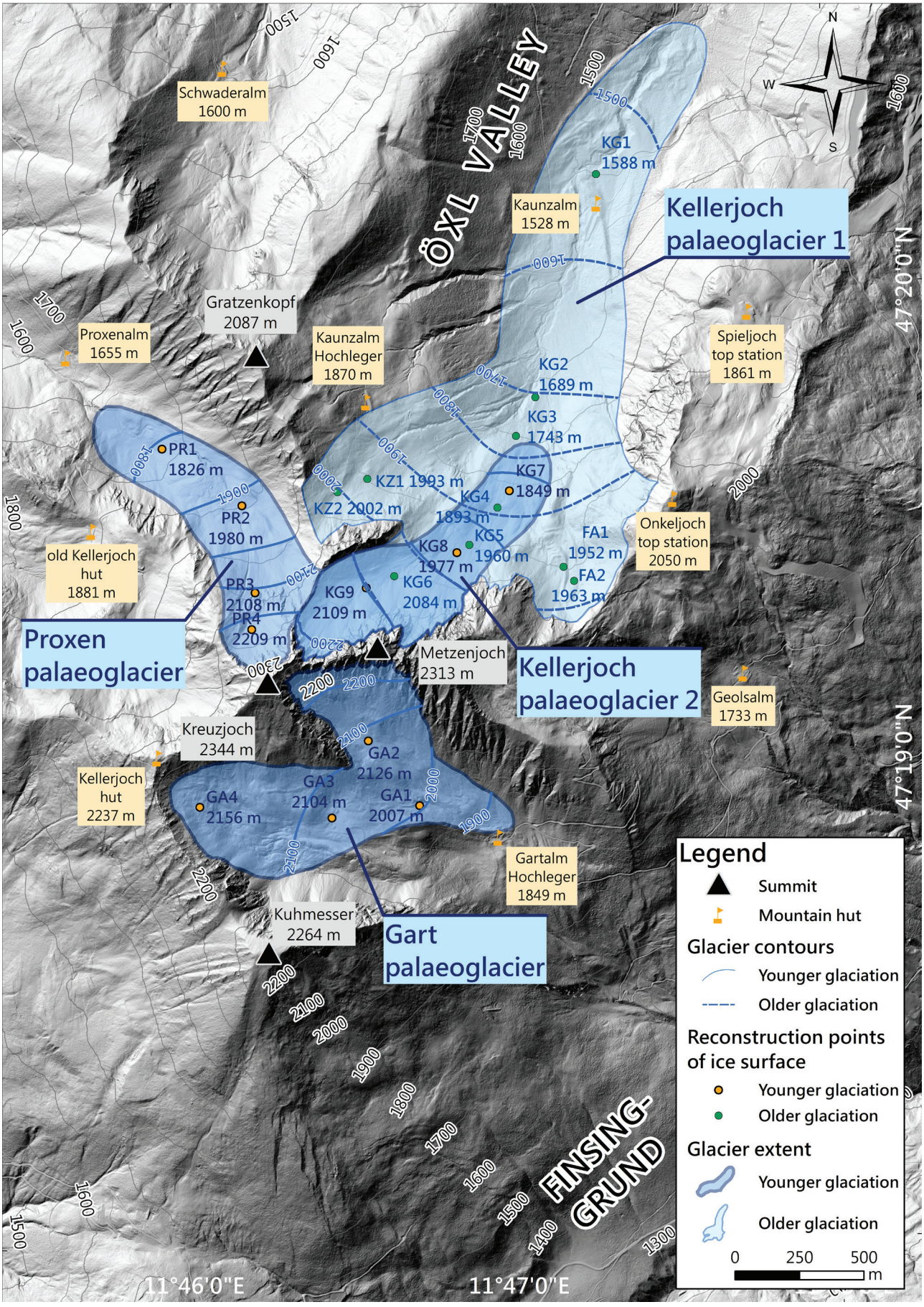

Figure 7: Reconstruction of Late Glacial palaeoglaciers in the Kellerjoch massif.

Table 2: Parameters of each calculation point for the ice thickness reconstruction of the studied palaeoglaciers. Grey shaded values show input parameters and other values were calculated from these. Shape factor values in italics were calculated using the Excel spreadsheet by Benn & Hulton (2010), while other values were transferred from appropriate cross sections.

Calculation point	Slope α [°]	tan α [ ]	Basal shear stress τ_0 [kPa]	Shape factor f' [ ]	Altitude [m a.s.l.]	Ice thickness H [m]	Ice surface [m a.s.l.]
Kellerjoch palaeoglacier 1							
KG1	6	0.105	50	*0.6*	1500	88	1588
KG2	18	0.325	125	*0.67*	1625	64	1689
KG3	18	0.325	125	1	1700	43	1743
KG4	10	0.176	100	1	1830	63	1893
KG5	22	0.404	130	0.6	1900	60	1960
KG6	15	0.268	125	*0.62*	2000	84	2084
FA1	15	0.268	75	0.6	1900	52	1952
FA2	25	0.466	100	*0.63*	1925	38	1963
KZ1	15	0.268	125	0.56	1900	93	1993
KZ2	30	0.577	150	*0.56*	1950	52	2002
Kellerjoch palaeoglacier 2							
KG7	23	0.424	130	1	1815	34	1849
KG8	24	0.445	130	0.6	1923	54	1977
KG9	18	0.325	125	0.62	2040	69	2109
Proxen palaeoglacier							
PR1	25	0.466	135	*0.63*	1775	51	1826
PR2	15	0.268	125	*0.65*	1900	80	1980
PR3	38	0.781	150	0.65	2075	33	2108
PR4	28	0.532	150	*0.6*	2157	52	2209
Gart palaeoglacier							
GA1	20	0.364	130	*0.67*	1948	59	2007
GA2	19	0.344	130	0.62	2058	68	2126
GA3	14	0.249	125	0.63	2016	88	2104
GA4	17	0.306	125	0.65	2086	70	2156

such as a steep frontal slope, elevated lateral ridges and in some cases also transverse ridges in the lower part and longitudinal ridges in the upper part. Slope angles of the front slope range from 32° to 40°. Except for the Kellerjochalm rock glacier, all others are covered by vegetation. Boulders up to several metres in diameter are present. The central part of the Kellerjochalm rock glacier also shows several circular depressions.

The largest rock glacier developed in front of the Falschegg glacier (Kellerjoch palaeoglacier 2) from sediment transported by the glacier. The boundary between glacier and rock glacier is difficult to determine, and the whole deposit is best described as a glacier-rockglacier continuum (Giardino and Vitek, 1988, Krainer and Mostler, 2000).

All rock glaciers developed in front of small glaciers or large firn patches from debris. Rock glaciers, which developed directly from scree slopes are missing. It should also be noted that in many places of the upper moraine sequence the moraines show more or less well developed rock glacier-like deformations, often similar to the deformation patterns of ice-cored moraines of sub-polar glaciers (Østrem 1964, 1971; Barsch, 1971). In total, those features show that permafrost existed down to an altitude of about 1750 m.

4.3.2 Other ridges

Three wall-like structures were identified in the study area (Fig. 3). Their morphologies are atypical compared to those of glacial moraines in the Kellerjoch area. About 400 m north of the Kaunzalm-Hochleger, a curved wall-like structure with a length of about 370 m and a height of a few metres lies beneath a short and steep slope. Its shape resembles a rounded W. Another ridge is present north of the Kuhmesser peak. This ridge shows larger dimensions, with a length of 500 m and a height of several metres. Further, this ridge clearly overlaps the most prominent, right-handed lateral moraine in the Gartalm cirque. A third wall-like structure is located in the Gartalm cirque. This ridge shows a length of about 200 m and has

Name	Length (m)	Width (m)	L/W	Classification (after Barsch, 1996)	Lowest altitude (m a.s.l.)	Highest altitude (m a.s.l.)
Falschegg	240	60	3.9	tongue-shaped	1870	1960
Schwaderalm	370	150	2.5	tongue-shaped	1655	1780
Proxenalm	200	80	2.4	tongue-shaped	1900	1990
Kellerjochalm	140	102	1.4	slightly tongue-shaped	2010	2090

Table 3: Parameters of the mapped rock glaciers.

a straight course. Transverse ridges can be also seen in the upper Falschegg cirque. They are between several metres and some tens of metres long and only a few metres in height. Most of them are curved resulting in an uneven topography in this cirque.

5 Discussion

5.1 Comparison of palaeo-ELA data

The combination of field mapping, results of the AAR and MELM methods and the calculation of former ice thickness yields a robust and rheologically plausible reconstruction of the former glacier cover in the study area (Fig. 7). The MELM-method as well as the AAR-Method in combination with morphological field evidence is a simple and powerful approach, especially when the field evidence is robust (i.e., well-developed lateral moraines and/or cirques) and glaciers are of more or less "normal" shape. But these approaches also involve potential errors. The present-day highest position of lateral moraines can be altered by erosion and/or by incomplete deposition of till. When applying the MELM-method to such an altered lateral moraine, the reconstructed ELA will be too low (Nesje and Dahl, 2000, Benn and Evans, 2010).

Gross et al. (1977) determined a typical AAR for alpine glaciers of 0.67. This value can be cross-checked with results from the MELM-method, provided that the lateral moraines were deposited in equilibrium with the local palaeoclimate and are not influenced by erosional processes mentioned above.

When the field evidence is robust and glaciers are of more or less "normal" shape, however, the AAR method provides a good means for estimating the palaeo-ELA. The results for the ELA reconstruction by both methods are in good agreement for the Proxen palaeoglacier and especially for the Kellerjoch palaeoglacier (Table 1). The difference of 30 m in case of the Proxen palaeoglacier may be due to the superposition of talus cones (Fig. 3). The determined ELAs at the Kellerjoch palaeoglacier only differ by about 10 m, which indicates no erosion of the lateral moraine.

The palaeo-ELA reconstruction of both methods yielded a discrepancy of 85 m at the Kellerjoch palaeoglacier 2. Three explanations appear possible: (1) The observed maximum altitude of the left-lateral moraine is too high. (2) The Kellerjoch palaeoglacier 2 also included the Falschegg cirque. The small AAR of 0.51 supports this assumption referring to a "typical alpine" AAR, despite lacking field evidence. (3) Field observations show that the lowest part of the glacier was debris-covered and developed into a rock glacier. If the debris-covered part is excluded from the glacier surface, the difference between the two methods is reduced to 10 m.

An inclusion of a palaeoglacier in the Falschegg cirque would result in an ELA of about 1925 m with an AAR of about 0.69. The geomorphology of the Falschegg cirque shows a slightly elevated ridge, which merges with the prominent right-lateral moraine of Kellerjoch palaeoglacier 2. This suggests a smaller palaeoglacier in the Falschegg cirque, which was connected to the main palaeoglacier tongue. During glacier retreat these two palaeoglaciers split, and the smaller Falschegg palaeoglacier continued to exist as a small cirque glacier. After this separation the latter formed the above mentioned ridge. This ridge closes the Falschegg cirque, supporting this interpretation. The reconstructed ELA considering this palaeoglacier extent yielded a value of about 1900 m and an AAR of 0.68. The first scenario considering only one main glacier tongue is preferred, but field evidence is ambiguous. The most realistic ELA of Kellerjoch palaeoglacier 2 is slightly less than 2000 m, as is indicated by the onset of the moraine and the reconstruction excluding the heavily debris-covered tongue.

For the Gartalm palaeoglacier the ELA reconstruction based on the MELM method yielded an altitude of 2010 m, whereas the MELM-method yielded an ELA value of 2060 m. Field evidence in the Gartalm cirque is robust, with a clearly definable ablation zone and a well-defined cirque which comprises the accumulation zone. Considering this and a superposition of the most prominent right-lateral moraine by a massive ridge, the estimate by the MELM-method appears too low.

Another interesting issue in the Gartalm cirque is the unusual position of the most prominent lateral moraine. Typically – e.g. in the case of the Kellerjoch palaeoglacier – a valley palaeoglacier forms lateral moraines symmetrically on both valley flanks. This is not the case for the Gartalm palaeoglacier, whose right-lateral moraine is located rather in the centre of this small valley. One explanation might be a medial moraine, which is typically deposited

	Locality	*Altitude of terminal moraine (m a.s.l.)*	*ELA (m a.s.l.)*	*Exposition*
younger glaciation	Larstig valley (Ivy-Ochs et al., 2009)	~ 2000	~ 2480	N
	Verwall Mountains (Sailer & Kerschner, 1999)	-	~ 2300	SE, NW
	Mieming Mountains (Moran et al., 2016a)	-	~ 1900-1950	N
	Southern Karwendel Mountains (Moran et al., 2016b)	~ 1600	~ 1990	N-NW
	Kellerjoch palaeoglacier 2 (this study)	**~ 1700 (estimated)**	**~ 1905**	**NNE**
	Proxen palaeoglacier (this study)	**~ 1680**	**~ 1870**	**NNW**
	Gart palaeoglacier (this study)	**~ 1850**	**~ 2060**	**ESE**
older glaciation	Trins, Gschnitz valley (Ivy-Ochs et al., 2006)	~ 1200	~ 1930	NE
	Möslalm, Karwendel Mountains (Kerschner, 1993)	-	~ 1710	N
	Gerlos Pass area, Ziller Valley (Patzelt, 1975)	~ 1200	~ 1950	N
	Kellerjoch palaeoglacier 1 (this study)	**~ 1420**	**~ 1660**	**NNE-NE**

Table 4: Selection of dated glacier advances in the Eastern Alps in the vicinity of the study area and their palaeoglaciological parameters. Values of this study were determined by the AAR-method.

at the confluence of two glaciers. The sediment of these medial moraines is in most cases transported on the glacier surface but does not show a high preservation potential. Considering also the lack of two sufficiently large confluent palaeoglaciers, this model appears unlikely. A more likely explanation for this central moraine ridge involves the Kuhmesser DSGSD (see section 5.2).

5.2 Retro-deformation of the Kuhmesser DSGSD

This DSGSD was investigated by Grasbon (2001), who placed the boundary of the DSGSD behind the peak of the Kuhmesser, suggesting that the entire peak is part of this DSGSD. This model provides a possible solution for the atypical geomorphological situation in the Gartalm cirque (section 5.1). The direction of movement of the Kuhmesser DSGSD is poorly known, but field observations allow to constrain its approximate path. The Finsingbach valley (in which the Kuhmesser-DSGSD is sagging) shows a kink on the western border of the DSGSD, whereas a straight continuation exists on the eastern border (Fig. 3). This leads to the assumption that sagging of this DSGSD occurs via a clockwise rotation with higher rates in the east and lower ones in the west, because the kink could act as a resistance. By retro-rotating the Kuhmesser-DSGSD about 150-200 m anti-clockwise, it almost perfectly fits the present-day right-lateral moraine of the Gartalm palaeoglacier. In this retro-deformed position, the Kuhmesser peak forms the right boundary to this palaeoglacier, and its lateral moraine is in valley-symmetrical position. Assuming an onset of the sagging during the deglaciation prior to the Gschnitz stadial (i.e. about 18-19 ka BP) results in a deformation rate of about 10 mm/a. This is a typical value for DSGSDs in the Alps (Crosta et al., 2008 a, b; Agliardi et al., 2012; Agliardi et al., 2013; Crosta et al., 2013). Using this retro-deformed topography, the MELM-method yields an ELA of about 2060 m, which matches the AAR-based ELA reconstruction. Observations supporting the mass movement model are very wide ridges beneath the Gartalm hut. These curved ridges have a central location similar to the prominent right-lateral moraine and could belong to an earlier glacier advance, possibly Gschnitz. Also, the divergent morphology of theses ridges could originate from the progressively increasing space provided by the Kuhmesser DSGSD.

5.3 Chronological correlation

In the absence of numerical ages, there are basically two main approaches for the stratigraphical assignment of moraines to an established stratigraphic scheme. Traditionally, the vertical distance between the ELA of a glacier

and a reference level (ELA depression) can be used as a guideline (Penck and Brückner, 1909; summary by Maisch, 1987). This approach assumes that glacier advances of similar age showed similar ELA depressions. However, the ELA depression as a climatic variable depends on both accumulation and ablation and is spatially variable. If a reference altitude, e.g. the Little Ice Age (LIA) ELA is missing, the method reaches its limit.

The sequence approach (e.g. Heuberger, 1966; Schoeneich, 1998; Reitner et al., 2016) assumes that sequences found in one region can be transferred to other regions. ELA depressions play only a secondary role if at all, and numerical ages can be used as anchor points for the interpolation of undated moraine sets. However, if moraine series in a certain valley are incomplete, the approach reaches its limit.

A further possibility is to distinguish moraines on the basis of their morphology, e.g. fresh moraines vs. moraines reworked by periglacial processes (e.g. Heuberger, 1966; Kerschner, 1978). The basic idea is that important morphological boundaries mark important stratigraphic boundaries.

Here we tried a combination of an ELA-based classification and the sequence approach, and we compared the available information with results in the vicinity of the study area. Table 4 shows selected localities which were chosen based on similar comparable parameters such as altitude and exposition.

In the study area, two sets of moraines can be distinguished, which themselves consist of a number of individual moraines and rock glaciers. Our system is very similar to the sequence established by Patzelt (2019), but we interpret some of his moraines as rock glaciers, and we favour a different stratigraphic assignment of the moraines. The older set of three successive moraines is only preserved in the Öxl valley (Kellerjoch palaeoglacier 1) and no corresponding geomorphological features were found in the rest of the study area. Three palaeoglaciers (Kellerjoch palaeoglacier 2, Proxen palaeoglacier and Gart palaeoglacier) were reconstructed for the younger glaciation.

5.3.1 Older glaciation

In his study of the Kellerjoch area, Patzelt (2019) used the LIA ELA of the former glacier at Rosenjoch, about 25 km to the Southwest of Kellerjoch, as a reference altitude for the calculation of ELA depressions which was determined at 2650 m (Patzelt, 1983). Hence he calculated an ELA-depression of almost 1000 m for the lowest moraine system at Kaunzalm. The ELA depressions for the rest of the Kaunzalm moraines are not much smaller. Consequently, he assigned the Kaunzalm moraines to the phase of Early Late Glacial Ice Decay (ELID, Reitner, 2005, 2007). Klebelsberg (1951), who implicitly assumed the local modern "snowline" (ELA) as 2600 m, assigned the Kaunzalm moraines to the "Schlern" stadial. The moraines higher up were assigned to the Gschnitz stadial (in the sense of the 1950s) by Klebelsberg (1951) and to the Gschnitz stadial in its present meaning by Patzelt (2019). Consequently, and in comparison with moraines in the Rofan Mountains north of the Inn valley, Patzelt (2019) assigned all moraines in the Kellerjoch massif to the pre-Bølling period of the Alpine Late Glacial and furthermore suggested it as a type region for the ELID phase of glacier recession outside and above the downwasting glaciers in the main valleys.

Here we suggest a different approach arguing that a LIA ELA of 2650 m for the reference altitude is too high for the Kellerjoch region. Compared to the Rosenjoch area southeast of Innsbruck, the Kellerjoch massif is much more open and exposed to the North via the Achensee valley and the Brandenberg Mountains. The peaks of the latter group are about as high as the cirque floors of the Kellerjoch. In the Riss valley (Karwendel Mountains) about 17 km to the NW, the ELA of small LIA glaciers was around 2200 m. Even if this is a very low ELA in a favourable position (Kuhn, 1993), it shows that a (virtual) LIA ELA of the Kellerjoch region may have been well below 2650 m.

According to Reitner et al. (2016), the Gschnitz stadial represents the first independent glacier advance following the ELID in the Eastern Alps. The traces of the ice decay in form of many terraces at varying altitudes can be observed near the mouth of the Öxl valley passing into the Ziller Valley. Although the Öxl valley above the entrance into the gorge is well suited for the preservation of moraines, there are no such deposits up to the Kaunzalm moraines. If we follow the sequence approach, the Kaunzalm moraines represent the Gschnitz stadial and at least the lowermost moraine should have been deposited around 16.5 ka BP (Ivy-Ochs et al., 2006; Kerschner et al., 2014). If we consider the Kaunzalm moraines A – C of Patzelt (2019) as a coherent series, its ELAs cover a range of 1650 to 1800 m. For the frontal set, the ELA is about 300 m lower than at the type locality in the central alpine Gschnitz valley and also 300 m lower than similar moraines in the Gerlos Pass region to the SE (Patzelt 1975). In the Karwendel Mountains to the NW, similar glacier extents had ELAs of about 1500 – 1550 m in the central mountain chain (H. Kerschner, unpubl. data) and about 1700 m in the southern mountain chain (Kerschner, 1993, see also Table 4). If our hypothesis is correct, the ELAs of the Kaunzalm glaciers would occupy an intermediate position between the Karwendel Mountains to the Northwest and the central Alps to the South. The ELA reconstructed for the palaeoglaciers in the Karwendel Mountains and the Kellerjoch region are comparable, while those from the Gerlos Pass and the Gschnitz valley are higher. Higher ELAs in the more central part of the mountains are consistent with the drier climate of the central Eastern Alps as compared to the northern rim of the Alps.

5.3.2 Younger glaciation

The younger, upper set of moraines includes all moraines in the study area with the exception of Kaunzalm A – C. It is not entirely clear for the moraines at Proxenalm (section 4.1.3) which Patzelt (2019) correlated with the

Kaunzalm B moraine, but an ELA of 1870 m puts them closer to the younger moraines in the Öxl valley. The ELAs of the younger moraines are in the range of 1900 – 2000 m. Palaeoglaciological parameters of the younger glaciation in the Kellerjoch region show larger differences when compared to reference localities (Table 4). An unambiguous correlation to known glacier advances is currently not possible. Patzelt (2019), based on ELA depressions, assigned the upper set of moraines to the Gschnitz stadial. Following the sequence approach, the upper set of moraines and rock glaciers should represent the Egesen stadial (Younger Dryas) and the tripartite moraine series identified at the Kellerjoch palaeoglacier 2 and the Gart palaeoglacier should have been deposited during the Egesen stadial. Also, the occurrence of fossil rock glaciers close to these moraines – they often also originated from them – supports this correlation (cf. Moran et al., 2016 a, b). On the other hand, the ELA difference between the older and the younger glaciation in the Kellerjoch region is only about 300 m, which appears rather small for a correlation with the Egesen glacier advance in comparison with central Alpine localities, where a difference of about 500 m is more typical. Moran et al. (2016 a, b) studied glacier advances in the Mieming and the Karwendel Mountains. There, the ELA of the Egesen maximum advance was between 1900 m and 1990 m. In the north-facing valleys of the central Karwendel Mountains, the ELAs of likely Egesen glaciers were between 1720 m and 1840 m (H. Kerschner, unpubl. data) and the difference to likely Gschnitz stadial ELAs is about 300 m. Thus, a correlation of the upper set of moraines and rock glaciers with the Egesen Stadial is a distinct possibility.

For the Gartalm cirque, Patzelt (2019) used two different ELA references for the strongly pronounced northern and southern orientation beneath the Kuhmesser and the Kreuzjoch. He correlated a highly eroded moraine series below the Gartalm hut with the moraine series at the Kaunzalm. A wall-like structure beneath the Kuhmesser peak was assigned to the Gschnitz stadial by Patzelt (2019). The same wall-like structure was earlier described as a mainly morainal landscape by Klebelsberg (1951). We favour an alternative interpretation of the geomorphological situation in the Gartalm cirque (see sections 5.2 and 5.4).

5.4 Pronival ramparts, solifluction features and rock glaciers

Wall-like structures described in section 4.3.2 are interpreted as pronival ramparts (Fig. 3). These structures form adjacent to perennial snow patches, where small rockfalls slide over the snow surface and are deposited near the rim. This process generates wall-like structures that are by definition a nival and not a glacial phenomenon. However, these processes may overlap, rendering the identification of pronival ramparts ambiguous in places (Hedding, 2016; Shakesby, 1997). Transverse ridges in the upper Falschegg cirque are attributed to solifluction, indicating permafrost-related soil movement after the disappearance of glacial ice in the study area. Patzelt (2019) consistently classified these rock glaciers as lateral moraines. Especially in the case of Falschegg, Proxenalm and Kellerjochalm, however, the geomorphological appearance strongly suggests that they formed as rock glaciers.

6 Conclusions

Detailed fieldwork aided by DEMs allowed to decipher the Late Glacial landscape history of the Kellerjoch region. Lateral and terminal moraines are distinct morphological features near the crest of this massif. In addition, fossil rock glaciers and pronival ramparts are present, which indicate permafrost activity after the ice glaciers had disappeared.

The most impressive moraine system is present near the Kaunzalm in the Öxl valley. Terminal moraines of this tripartite system are located at 1420 m, 1480 m and 1500 m. Right-lateral moraine ridges are well developed, whereas the left-lateral moraines are more subtle. Right-lateral moraine ridges can be traced to 1660 m, allowing to reconstruct the ELA at this elevation. A comparison with dated localities in the Eastern Alps suggests that this glacier advance corresponds to the Gschnitz stadial (16-17 ka BP).

A younger glaciation closer to the Kellerjoch crest was identified as Kellerjoch palaeoglacier 2, Proxen palaeoglacier and Gart palaeoglacier. At Kellerjoch palaeoglacier 2 and Gart palaeoglacier a tripartite moraine series was identified, whereas at Proxen palaeoglacier only one distinct moraine is present. Lowest terminal moraines are located at 1700 m, 1850 m and 1680 m, respectively, and the ELAs were reconstructed at 1905 m, 2060 m and 1870 m, respectively. A correlation of this younger moraine system to the Egesen stadial is likely but not proven. Future studies should attempt to date these morphological features to better constrain their timing. Rock glaciers near the Kellerjoch crest commonly evolved from terminal moraines as well as talus deposits, suggesting a near-contemporaneous existence of ice glaciers and rock glaciers.

We confirm the Grasbon (2001) model which explains the unusual position of a moraine ridge in a valley-central position. Retro-deforming the displacement by the DSGSD since the LGM yields a plausible position of the former Kuhmesser peak and provides a solution for the atypical location of the prominent lateral moraine at Gartalm.

Acknowledgements

Digital elevation models were kindly provided by the Government of Tyrol at a resolution of 1 m. We are grateful to T. Bartosch and J. Reitner for their helpful comments on an earlier version and K. Stüwe for editorial support.

References

Agliardi, F., Crosta, G.B., Frattini, P., 2012. Slow rock-slope deformation. In: Clague, J.J. and Stead, D. (eds.), Landslides: Types, mechanisms, and modeling. Cambridge University Press, Cambridge, pp. 207–221.

Agliardi, F., Crosta, G.B., Frattini, P., Malusà, M.G., 2013. Giant non-catastrophic landslides and the long-term exhumation of the European Alps. Earth and Planetary Science Letters 365, 263–274. https://doi.org/10.1016/j.epsl.2013.01.030.

Auer, I., Foelsche, U., Böhm, R., Chimani, B., Haimberger, L., Kerschner, H., Koinig, K.A., Nicolussi, K., Spötl, C., 2014. Vergangene Klimaänderung in Österreich. In: Österreichischer Sachstandsbericht Klimawandel 2014 (AAR14). Austrian Panel on Climate Change (APCC), Verlag der Österreichischen Akademie der Wissenschaften, Wien, 227–300.

Balco, G., Briner, J., Finkel, R.C., Rayburn, J.A., Ridge, J.C., Schaefer, J.M., 2009. Regional beryllium-10 production rate calibration for late-glacial northeastern North America. Quaternary Geochronology 4, 93–107. https://doi.org/10.1016/j.quageo.2008.09.001.

Barsch, D., 1971. Rock glaciers and ice-cored moraines. Geografiska Annaler Ser. A 53, 203-206.

Barsch, D., 1996. Rockglaciers. Indicators for the present and former geoecology in high mountain environments. Springer, Berlin.

Benn, D.I., Evans, D.J.A., 2010. Glaciers & Glaciation. 2nd edition. Routledge, London.

Benn, D.I., Hulton, N.R.J., 2010. An ExcelTM spreadsheet program for reconstructing the surface profile of former mountain glaciers and ice caps. Computers & Geosciences 36, 605–610. https://doi.org/10.1016/j.cageo.2009.09.016.

Bortenschlager, S., 1984. Beiträge zur Vegetationsgeschichte Tirols I. Inneres Ötztal und unteres Inntal. Berichte des naturwissenschaftlich-medizinischen Vereins Innsbruck 71, 19–56.

Crosta, G.B., Allievi, J., Frattini, P., Giannico, C., Lari, S., 2008a. Monitoring deep-seated gravitational slope deformations in the Alps by PSInSAR techniques. Geophysical Research Abstracts 10, EGU2008-A-10662.

Crosta, G.B., Agliardi, F., Frattini, P., Zanchi, A., 2008b. Alpine inventory of deep-seated gravitational slope deformations. Geophysical Research Abstracts 10, EGU2008-A-02709.

Crosta, G.B., Frattini, P., Agliardi, F., 2013. Deep seated gravitational slope deformations in the European Alps. Tectonophysics 605, 13–33. https://doi.org/10.1016/j.tecto.2013.04.028.

Cuffey, K.M. and Paterson, W.S.B., 2011. The physics of glaciers. 4th ed. Butterworth-Heinemann, Burlington, MA, 693 pp.

Finsterwalder, S., 1897. Der Vernagtferner – seine Geschichte und seine Vermessung in den Jahren 1888 und 1889, Wissenschaftliche Ergänzungshefte zur Zeitschrift des Deutschen und Österreichischen Alpenverein, 1. Verlag Dt. u. Österr. Alpenverein, Graz.

Gild, C., Geitner, C., Sanders, D., 2018. Discovery of a landscape-wide drape of late-glacial aeolian silt in the western Northern Calcareous Alps (Austria): First results and implications. Geomorphology 301, 39–52. https://doi.org/10.1016/j.geomorph.2017.10.025.

Grasbon, B., 2001. Großmassenbewegungen im Grenzbereich Innsbrucker Quarzphyllit, Kellerjochgneis, Wildschönauer Schiefer, Finsinggrund (Vorderes Zillertal). Unpublished Diploma thesis, University of Innsbruck.

Gross, G., Kerschner, H., Patzelt, G., 1977. Methodische Untersuchungen über die Schneegrenze in alpinen Gletschergebieten. Zeitschrift für Gletscherkunde und Glazialgeologie 12, 223–251.

Haditsch, G., Mostler, H., 1982. Zeitliche und stoffliche Gliederung der Erzvorkommen im Innsbrucker Quarzphyllit. Geologisch-Paläontologische Mitteilungen Innsbruck 12, 1–40.

Hedding, D.W., 2016. Pronival ramparts. Progress in Physical Geography 40, 835–855. https://doi.org/10.1177/0309133316678148.

Heuberger, H. 1966. Gletschergeschichtliche Untersuchungen in den Zentralalpen zwischen Sellrain- und Ötztal. Wissenschaftliche Alpenvereinshefte 20, 1-125.

Heiri, O., Koinig, K.A., Spötl, C., Barrett, S., Brauer, A., Drescher-Schneider, R., Gaar, D., Ivy-Ochs, S., Kerschner, H., Luetscher, M., Moran, A., Nicolussi, K., Preusser, F., Schmidt, R., Schoeneich, P., Schwörer, C., Sprafke, T., Terhorst, B., Tinner, W., 2014. Palaeoclimate records 60–8 ka in the Austrian and Swiss Alps and their forelands. Quaternary Science Reviews 106, 186–205. https://doi.org/10.1016/j.quascirev.2014.05.021.

Heyman, J., 2014. Paleoglaciation of the Tibetan Plateau and surrounding mountains based on exposure ages and ELA depression estimates. Quaternary Science Reviews 91, 30–41. https://doi.org/10.1016/j.quascirev.2014.03.018.

Ivy-Ochs, S., 2015: Glacier variations in the European Alps at the end of the last glaication. Cuadernos de Investigación Geográfica 41, 295-315. DOI: 10.18172/cig.2750.

Ivy-Ochs, S., Kerschner, H., Kubik, P.W., Schlüchter, C., 2006. Glacier response in the European Alps to Heinrich Event 1 cooling: The Gschnitz stadial. Journal of Quaternary Science 21, 115-130. https://doi.org/115–130.10.1002/jqs.955.

Ivy-Ochs, S., Kerschner, H., Schlüchter, C., 2007. Cosmogenic nuclides and the dating of Lateglacial and Early Holocene glacier variations: The Alpine perspective. Quaternary International 164-165, 53–63. https://doi.org/10.1016/j.quaint.2006.12.008.

Ivy-Ochs, S., Kerschner, H., Reuther, A., Preusser, F., Heine, K., Maisch, M., Kubik, P.W., Schlüchter, C., 2008. Chronology of the last glacial cycle in the European Alps. Journal of Quaternary Science 23, 559–573. https://doi.org/10.1002/jqs.1202.

Ivy-Ochs, S., Kerschner, H., Maisch, M., Christl, M., Kubik, P.W., Schlüchter, C., 2009. Latest Pleistocene and Holocene glacier variations in the European Alps. Quaternary Science Reviews 28, 2137–2149. https://doi.org/10.1016/j.quascirev.2009.03.009.

Kerschner, H. 1978. Untersuchungen zum Daun- und Egesenstadium in Nordtirol und Graubünden (methodische Überlegungen). Geographischer Jahresbericht aus Österreich 36, 26-49.

Kerschner, H., 1993. Späteiszeitliche Gletscherstände im südlichen Karwendel bei Innsbruck, Tirol. Innsbrucker Geographische Studien 20, 47–55.

Kerschner, H., Ivy-Ochs, S., 2008. Palaeoclimate from glaciers: Examples from the Eastern Alps during the Alpine Lateglacial and early Holocene. Global and Planetary Change 60, 58–71. https://doi.org/10.1016/j.gloplacha.2006.07.034.

Kerschner, H., Ivy-Ochs, S., Schlüchter, C., 1999. Paleoclimatic interpretation of the early late-glacial glacier in the Gschnitz valley, Central Alps, Austria. Annals of Glaciology 28, 135–140.

Kerschner, H., Ivy-Ochs, S., Schlüchter, C., 2008. Gletscher und Klima im Ostalpenraum zwischen 16.000 und 11.000 Jahren vor heute. In: Reitner, J.M. (ed.), Veränderter Lebensraum: Gestern, heute, morgen; Tagung der Deutschen Quartärvereinigung e.V. 31. August - 6. September 2008 Universität für Bodenkultur Wien. Geologische Bundesanstalt, Vienna.

Kerschner, H., Ivy-Ochs, S., Terhorst, B., Damm, B., Ottner, F., 2014. The moraine at Trins - type locality of the Gschnitz Stadial. In: Kerschner, H., Krainer, K., Spötl, C. (eds.), From the foreland to the Central Alps: Field trips to selected sites of Quaternary research in the Tyrolean and Bavarian Alps. Geozon, Berlin, 100–105.

Klasen, N., Fiebig, M., Preusser, F., Reitner, J.M., Radtke, U., 2007. Luminescence dating of proglacial sediments from the Eastern Alps. Quaternary International 164-165, 21–32. https://doi.org/10.1016/j.quaint.2006.12.003.

Klebelsberg, R., 1951. Gletscher am Kellerjoch. Schlern-Schriften 85, 59-66.

Kolenprat, B., Rockenschaub, M., Frank, W., 1999. The tectonometamorphic evolution of Austroalpine units in the Brenner Area (Tirol, Austria) - structural and tectonic implications. Tübinger Geowissenschaftliche Arbeiten 52, 116–117.

Krainer, K., Mostler, W., 2000. Reichenkar rock glacier: a glacier derived debris-ice system in the western Stubai Alps, Austria. Permafrost and Periglacial Processes 11, 267-275.

Kuhn, M., 1993. Zwei Gletscher im Karwendelgebirge. Zeitschrift für Gletscherkunde und Glazialgeologie 29, 85-92.

Lichtenecker, N., 1938. Die gegenwärtige und die eiszeitliche Schneegrenze in den Ostalpen. Verhandlungen der III. internationalen Quartär-Konferenz, Vienna 1936, 141–147.

Maisch, M. 1987. Zur Gletschergeschichte des alpinen Spätglazials: Analyse und Interpretation von Schneegrenzdaten. Geographica Helvetica 42, 63-71.

Moran, A.P., Ivy Ochs, S., Vockenhuber, C., Kerschner, H., 2016a. Rock glacier development in the Northern Calcareous Alps at the Pleistocene-Holocene boundary. Geomorphology 273, 178–188. https://doi.org/10.1016/j.geomorph.2016.08.017.

Moran, A.P., Ivy-Ochs, S., Vockenhuber, C., Kerschner, H., 2016b. First ^{36}Cl exposure ages from a moraine in the Northern Calcareous Alps. E&G Quaternary Science Journal 65, 145-155.

Moser, M., 2008. GEOFAST Karte Blatt 119 - Schwaz. Geologische Bundesanstalt, Vienna.

Nesje, A., Dahl, S.O., 2000. Glaciers and environmental change. Routledge, London, 203 pp.

Nye, J.F., 1952. The mechanics of glacier flow. Journal of Glaciology 2, 82-93.

Nye, J.F., 1965. The flow of a glacier in a channel of rectangular, elliptic or parabolic cross section. Journal of Glaciology 5, 661–690.

Østrem, G., 1964. Ice-cored moraines in Scandinavia. Geografiska Annaler Ser. A. 46, 282-337.

Østrem, G., 1971. Rock glaciers and ice-cored moraines. A reply to D. Barsch. Geografiska Annaler Ser. A 53, 207-213.

Patzelt, G., 1975. Unterinntal - Zillertal - Pinzgau - Kitzbühel: Spät- und postglaziale Landschaftsentwicklung. In: Fliri, F. and Leidlmair, A. (eds.), Tirol - Ein geographischer Exkursionsführer. Geographisches Institut der Universität Innsbruck, Innsbruck, 309–329.

Patzelt, G., 1983. Die spätglazialen Gletscherstände im Bereich des Mieslkopfes und im Arztal, Tuxer Voralpen, Tirol. Innsbrucker Geographische Studien 8, 35-44.

Patzelt, G., 2019. Gletscher: Klimazeugen von der Eiszeit bis zur Gegenwart. Hatje Cantz, Berlin, 255 pp.

Penck, A., Brückner, E., 1909. Die Alpen im Eiszeitalter Volume 1-3. Tauchnitz, Leipzig.

Piber, A., 2005. The metamorphic evolution of the Austroalpine nappes north of the Tauern Window (Innsbruck Quartzphyllite Complex - Patscherkofel Crystalline Complex - Kellerjochgneiss and Wildschönau Schists). Unpublished PhD thesis, University of Innsbruck.

Reitner, J.M., 2005. Quartärgeologie und Landschaftsentwicklung im Raum Kitzbühel - St. Johann i.T. - Hopfgarten (Nordtirol) vom Riss bis in das Würm-Spätglazial (MIS 6-2). Unpublished PhD thesis, University of Vienna.

Reitner, J.M., 2007. Glacial dynamics at the beginning of Termination I in the Eastern Alps and their stratigraphic implications. Quaternary International 164-165, 64–84. https://doi.org/10.1016/j.quaint.2006.12.016.

Reitner, J., Ivy-Ochs, S., Drescher-Schneider, R., Hajdas, I., Linner, M. 2016. Reconsidering the current stratigraphy of the Alpine Lateglacial: Implications of the sedimentary and morphological record of the Lienz area (Tyrol, Austria). E&G Quaternary Science Journal 65, 113-144.

Rockenschaub, M., Kolenprat, B., Frank, W., 1999. The tectonometamorphic evolution of Austroalpine units in the Brenner area (Tirol, Austria) - new geochronological implications. Tübinger Geowissenschaftliche Arbeiten 52, 118–119.

Sailer, R., Kerschner, H., 1999. Equilibrium-line altitudes and rock glaciers during the Younger Dryas cooling event, Ferwall group, western Tyrol, Austria. Annals of Glaciology 28, 141–145.

Schmidt, R., Weckström, K., Lauterbach, S., Tessadri, R., Huber, K., 2012. North Atlantic climate impact on early late-glacial climate oscillations in the south-eastern Alps inferred from a multi-proxy lake sediment record.

Journal of Quaternary Science 27, 40–50. https://doi.org/10.1002/jqs.1505.

Schoeneich, P., 1998. Les stades tardiglaciaires des Préalpes vaudoises et leur corrélation avec le modèle des Alpes oreientales. Mitteilungen VAW-ETH Zürich 158, 192-204.

Shakesby, R.A., 1997. Pronival (protalus) ramparts: a review of forms, processes, diagnostic criteria and palaeoenvironmental implications. Progress in Physical Geography 21, 394–418.

Tropper, P., Finger, F., Krenn, E., Klötzli, U., Piber, A., Gangl, S., 2016. The Kellerjoch Gneiss (Tyrol, Eastern Alps): An Ordovician pluton with A-type affinity in the crystalline basement nappes north of the Tauern Window. Austrian Journal of Earth Sciences 109, 178–188. https://doi.org/10.17738/ajes.2016.0013.

Tropper, P., Piber, A., 2012. Geothermobarometry of quartzphyllites, orthogneisses and greenschists of the Austroalpine Basement Nappes in the northern Zillertal (Innsbruck Quartzphyllite Complex, Kellerjochgneis, Wildschönau Schists; Tyrol, Eastern Alps). Austrian Journal of Earth Sciences 105, 80–94.

van Husen, D., 1987. Die Ostalpen und ihr Vorland in der letzten Eiszeit (Würm). Map 1 : 500,000, Austrian Geol. Survey, Vienna.

van Husen, D., 1997. LGM and late-glacial fluctuations in the Eastern Alps. Quaternary International 38-39, 109–118. https://doi.org/10.1016/S1040-6182(96)00017-1.

Visser, P.C., 1938. Wissenschaftliche Ergebnisse der Niederländischen Expeditionen in den Karakorum und die angrenzenden Gebiete in den Jahren 1922-1935. Volume II Glaziologie. E.J. Brill, Leiden, 216 pp.

Wirsig, C., Zasadni, J., Christl, M., Akçar, N., Ivy-Ochs, S., 2016. Dating the onset of LGM ice surface lowering in the High Alps. Quaternary Science Reviews 143, 37–50. https://doi.org/10.1016/j.quascirev.2016.05.001

Received: 11.11.2019
Accepted: 5.10.2020
Editorial Handling: Kurt Stüwe